CHAPTER 5

Photoexcitation in Pure and Modified Semiconductor Photocatalysts

GONU KIM[a], YISEUL PARK[a], GUN-HEE MOON[b], AND WONYONG CHOI*[b]

[a]Division of Nano and Energy Convergence Research, Daegu Gyeongbuk Institute of Science & Technology (DGIST), Daegu 711-873, Korea; [b]School of Environmental Science and Engineering, Pohang University of Science and Technology (POSTECH), Pohang 790-784, Korea
*E-mail: wchoi@postech.edu

5.1 Band-Gap Excitation of Semiconductor Photocatalysts

Semiconductor photocatalysis has been applied to various energy and environmental problems: it has been used for water splitting to produce hydrogen gas, CO_2 reduction, waste-water treatment, odor control, and synthesis of chemicals.[1–4] However, although there are numerous different semiconductors, only a few of them are suitable as practical photocatalysts. For a semiconductor to be an efficient photocatalyst, it should absorb as much solar energy as possible. Figure 5.1(a) shows the solar spectra and possible solar-energy absorption ranges of various semiconductors. Figure 5.1(b)

RSC Energy and Environment Series No. 14
Photocatalysis: Fundamentals and Perspectives
Edited by Jenny Schneider, Detlef Bahnemann, Jinhua Ye, Gianluca Li Puma, and Dionysios D. Dionysiou

Published by the Royal Society of Chemistry, www.rsc.org

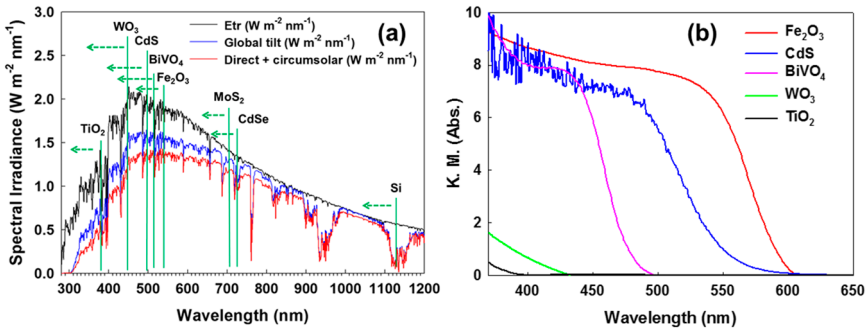

Figure 5.1 (a) Solar spectra and possible solar-energy absorption ranges of various semiconductors. The solar spectra were obtained from ASTM Standard G173-03 reference spectra. (b) Diffuse reflectance UV-visible spectra of semiconductors that are commonly employed as photocatalysts.

shows the diffuse reflectance UV-visible spectra of some widely used semiconductors. Wide band-gap semiconductors such as TiO_2 can absorb only a small portion (*i.e.*, the UV light region) of solar energy, while small band-gap semiconductors including Fe_2O_3, CdS, and Si can extend their absorption spectrum into the visible light region of solar energy. This absorption of solar energy is the first step of semiconductor photocatalysis to convert solar energy into chemical energy.

From the perspective of solar energy absorption, wide band-gap semiconductors are inefficient. However, most of the commercialized semiconductor photocatalysts are wide band-gap metal–oxide semiconductors, including TiO_2 (3.0–3.2 eV), WO_3 (2.8 eV), $SrTiO_3$ (3.2 eV), and ZnO (3.2 eV); this is because a sufficient band-gap energy or high oxidizing/reducing power is required to promote most of the useful redox reactions. For example, at least 1.23 V of energy is required to induce water splitting, and only wide band-gap semiconductors can absorb light with a higher energy than the required potential.[4] In the case of pollutant removal, a strong oxidizing/reducing power is also required. In addition, practical semiconductors should be (photo)chemically stable over long reaction periods; however, metal sulfides or iron oxides undergo photocorrosion or become inactive after a period of reaction time.[1] Therefore, stable metal-oxide semiconductors, such as TiO_2, that have large band-gaps have been widely investigated and proven to be suitable as practical photcatalysts.[5]

The photocatalytic process that occurs in pure semiconductors is schematically illustrated in Figure 5.2(a). Semiconductors consist of a filled valence band (VB) and an empty conducting band (CB) and can absorb light for various redox reactions. When light of energy greater than the band-gap of the semiconductor is illuminated onto the semiconductor, an electron from the VB is promoted to the CB, creating electron–hole pairs. The photogenerated electron–hole pair can recombine to release thermal energy. However, if the electron–hole pair is separated and transferred to the surface of

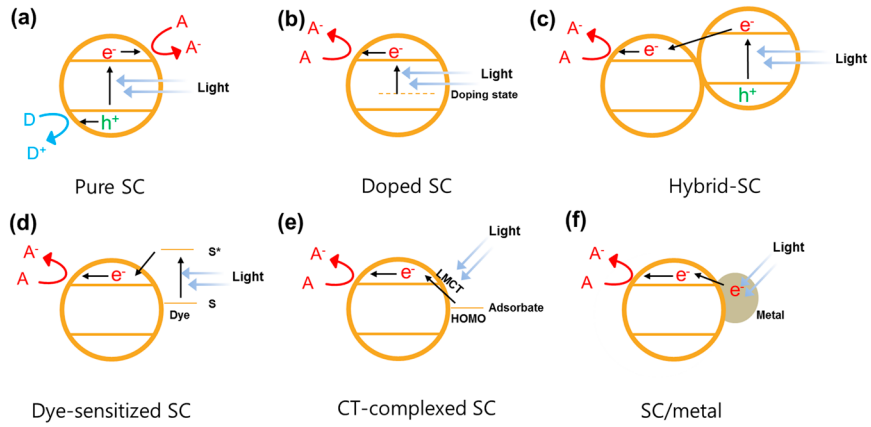

Figure 5.2 Schematics of photocatalysis processes in pure and modified semiconductors: (a) Pure SC, (b) Doped SC, (c) Hybrid-SC, (d) Dye-sensitized SC, (e) CT-complexed SC, (f) SC/metal (SC, semiconductor; A, electron acceptor; D, electron donor).

semiconductor, it can reduce and oxidize an adsorbate, assuming that the redox potential of the adsorbate is thermodynamically appropriate for the reaction. In such a process, the adsorbed electron donor is oxidized to form D^+ and the adsorbed electron acceptor is reduced to A^-.

However, no single semiconductors fulfill all the requirements for practical semiconductor photocatalysis (*i.e.*, visible light absorption, photostability, low cost, and abundance); thus, a variety of strategies have been developed to enhance the efficiency of semiconductor photocatalysts. For example, to enhance the light absorption of wide band-gap semiconductors, impurity doping, coupling with a semiconductor with a narrow band-gap, dye sensitization, ligand-to-metal charge transfer (LMCT) sensitization, and local surface plasmon resonance (LSPR)-sensitization techniques (Figure 5.2b–f) have been developed. Figure 5.3 shows the actual enhancement of the visible light absorption of TiO_2, which is a wide band-gap semiconductor, by using the above-mentioned techniques. These results demonstrate the utility of these methods for extending the light response of semiconductors. Compared with pure TiO_2, all the modified TiO_2 semiconductors exhibit significantly enhanced visible light absorption. However, each method has its own advantages and limitations, which will be discussed in detail in the following sections.[6–10]

5.2 Photoexcitation of Impurity-Doped Semiconductors

Doping by introducing foreign elements to the host materials is one of the most commonly used methods to reduce the band-gap of semiconductor photocatalysts. Upon doping with a foreign element, an intra-band state close to the CB or VB edge of the original band-gap can be introduced causing

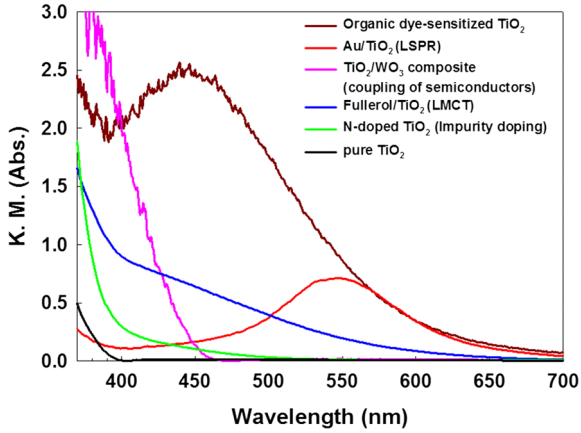

Figure 5.3 Diffuse reflectance UV-visible spectra of pure and modified TiO_2 samples. All samples were prepared according to the method described in the literature.[6–10]

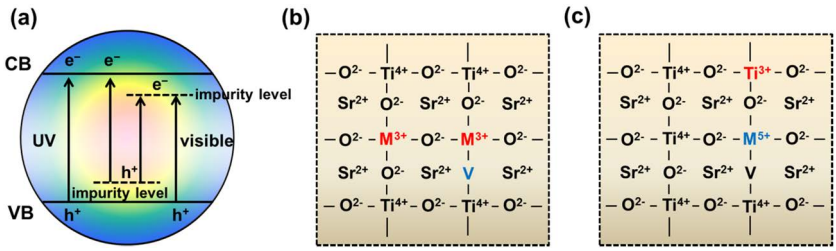

Figure 5.4 (a) Band-gap modification of semiconductors by doping with a foreign element. Schematic illustration of aliovalent-doped $SrTiO_3$: doping with a (b) trivalent cation and (c) pentavalent cation. (Adapted with permission.[12] Copyright 2009 American Chemical Society.)

a shift of the light absorption spectra to a longer wavelength (Figure 5.4a). To date, various doping strategies such as metal/non-metal ion doping, co-doping with different ions, and self-doping have been developed to enhance the band-gap absorption of the visible light region. Owing to its high reactivity and chemical stability, TiO_2 is the most investigated host material for doping.

Various kinds of metal ions, such as Fe^{3+}, Cr^{3+}, Co^{3+}, Mn^{3+}, V^{4+}, and Mo^{5+}, have been introduced to make TiO_2 visible-light active. Metal ions with similar ionic radii to that of Ti^{4+} are easily doped into the TiO_2 lattice resulting in the formation of new energy levels within the band-gap of TiO_2. Metal dopants, including V^{4+}, Mn^{3+}, and Co^{3+}, can generate an energy level below the CB of TiO_2, acting as trapping centers for electrons. In contrast, dopants such as Fe^{3+} and Cr^{3+} form energy levels above the VB of TiO_2, which can trap holes. The formation of intrinsic defects (such as oxygen vacancies and interstitial Ti) by doping also enhances the visible-light absorption.[11,12] As shown in Figure 5.4(b), trivalent cation (M^{3+}) dopants can occupy the Ti^{4+} sites as lower

valence cations resulting in the formation of oxygen vacancies. In contrast, pentavalent cation (M^{5+}) dopants occupying Ti^{4+} sites would cause the formation of Ti^{3+}, which inhibits the formation of oxygen vacancies (Figure 5.4c). Electrons located in the oxygen vacancy states directly affect the electronic structure of TiO_2 by forming a donor level below the CB.[13] The energy level that originates from oxygen vacancies has been reported to be located ~0.75–1.18 eV below the CB of TiO_2. In addition, Ti^{3+} defects can generate a shallow donor level just below the CB, which could also contribute to the visible-light response.[13] These new energy levels can take part in a new photoexcitation process. The electron can be excited to the oxygen vacancy states from the VB under visible light. For this reason, oxygen vacancies are called F centers, from "farbe", which is the German word for color. In addition to extending the light-absorption range of TiO_2, the energy levels that are induced by doping may serve as a trap site of electrons to inhibit electron–hole pair recombination. However, conversely, the dopant-induced defects formed in TiO_2 may reduce the photo-activity by serving as a recombination center at higher doping concentrations.[14–16] Therefore, the optimum doping concentration in metal ion-doped TiO_2 is usually low (typically 0.5–1.0%).[14,17–20] In addition, it should be realized that the electrons and holes trapped at the dopant sites are less energetic than free carriers in their reductive and oxidative potential, respectively.

Since Asahi *et al.* reported the enhanced photocatalytic activity of N-doped TiO_2 under visible-light irradiation,[21] various non-metal (*e.g.*, C, S, B, P, or F)-doped TiO_2 systems have been investigated.[22–28] Although all these non-metal-doped TiO_2 have been reported to induce visible-light photocatalytic reactivity, the explanation for the origin of visible-light absorption is under debate. The following proposals have been made: (i) N 2p states mixed with O 2p states result in a transition from the N $2p_\pi$ to Ti d_{xy} instead of from O $2p_\pi$, which leads to visible-light absorption.[21] (ii) The isolated N 2p states above the VB of TiO_2 are responsible for visible-light absorption in N-doped TiO_2.[29] (iii) N-doped anatase TiO_2 with different doping levels has similar photon transition energies, while localized N 2p states form above the VB at lower doping levels, and the N 2p states mix with O 2p states at high doping levels.[30,31] (iv) Oxygen vacancies induced by N doping contribute to absorption as well as the photocatalytic activity in the visible region, similar to the case in metal ion-doped TiO_2 systems.[32–34]

As an alternative to metal or non-metal doping, co-doping is a more attractive method that could result in higher photocatalytic activities and more beneficial characteristics than mono-doped TiO_2. TiO_2 co-doped with different dopant ions has new energy levels within the TiO_2 band-gap that originate from both dopant ions. Therefore, a narrower band-gap than that of mono-doped TiO_2 can form leading to stronger visible light absorption. In addition to the benefits of band-gap narrowing, co-doping can also effectively increase the number of dopant atoms that are incorporated into the lattice of the host materials *via* the charge compensation effect.[35] Co-doping can also effectively suppress the formation of recombination centers

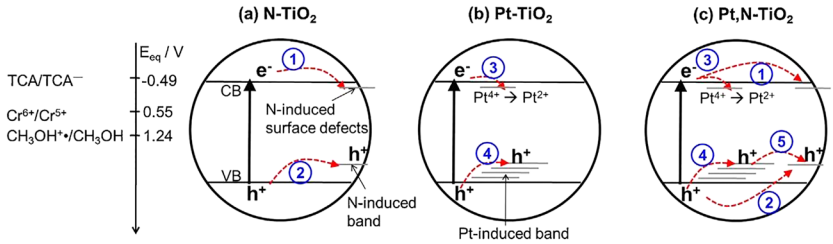

Figure 5.5 Schematic illustration of electron and hole trapping in (a) N–TiO_2, (b) Pt–TiO_2, and (c) Pt,N–TiO_2 under 355 nm irradiation. The numbers refer to the following charge-transfer steps: (1) electron trapping on the defect site, (2) hole trapping on the N-induced state, (3) intervalent charge transfer or conversion of Pt^{4+} into Pt^{2+}, (4) localization of holes on the Pt-induced band, and (5) hole-hopping. For comparison, the one-electron reduction potentials of the tested substrates are shown on the left-hand side. (Adapted with permission.[9] Copyright 2014 Elsevier.)

and promote charge separation, thus improving the photocatalytic performance. For example, co-doping with Pt and N enhances visible-light absorption and the photocatalytic conversion efficiency under visible light.[9] Such synergistic effects are attributed to the Pt- and N-induced mid-gap levels in which charge pairs are effectively separated. The new mid-gap levels created by co-doping affect hole trapping while the Pt transition ($Pt^{4+} \rightarrow Pt^{2+}$) dominantly contributes to electron trapping in Pt,N–TiO_2 (Figure 5.5). Therefore, the electronic interactions between Pt and N in co-doped TiO_2 facilitate charge-carrier mobility and reduce charge recombination, resulting in photocatalytic synergy.

The intrinsic point defects (*i.e.*, oxygen vacancies, titanium vacancies, and interstitial titanium) that affect the electronic structure of doped semiconductors also affect the visible-light absorption and photocatalytic activity.[36,37] Oxygen vacancies and Ti interstitials form donor levels 0.75–1.18 and 1.23–1.56 eV below the CB, respectively, while Ti vacancies give rise to acceptor levels above the VB.[36] These defects can induce an additional shoulder absorption band in the visible-light range or a tail absorption band in the near-infrared region depending on the preparation procedures. For instance, the optical absorption of hydrogenated TiO_2 nanocrystals shifts from UV to near-infrared, which is accompanied by a dramatic color change of the TiO_2 sample from white to black. The band-gap of hydrogenated black TiO_2 is about 1.0–1.8 eV, indicating that this material can absorb visible and even infrared photons for photocatalysis.[38,39]

5.3 Photoexcitation of Coupled Semiconductors

Various composite photocatalysts have been developed by coupling different semiconductors to enhance the photocatalytic efficiency in terms of effective charge separation and solar-light absorption.[40] The built-in potential

induced by the contact of semiconductors with different band positions can facilitate interfacial charge transfer, which can efficiently prohibit the recombination of photogenerated charge carriers.

All semiconductors in a composite can be concurrently excited when the illuminated light has sufficient energy to excite all the semiconductors (Figure 5.6a). Photogenerated electrons migrate from CB1 to CB2 and holes migrate from VB2 to VB1; thus, electrons and holes are effectively separated. Accordingly, more electrons and holes on semiconductor 2 (Semi-2) and semiconductor 1 (Semi-1), respectively, are available for photo-redox reactions. Photo-excitation of solely Semi-1 induces electron transfer from CB1 to CB2 (Figure 5.6b) and potential further transfer to CB3 (Figure 5.6c), while the holes of VB1 remain, which can retard the recombination of the charge carriers (*e.g.*, in CdS/TiO_2, Bi_2S_3/TiO_2, PbS/TiO_2, and $CdS/TiO_2/WO_3$).[41–44] However, one obvious drawback of these composites is that the redox potential of the transferred electrons and holes is greatly reduced resulting in decreased redox power. From this perspective, the Z-scheme has the merit of maintaining electrons/holes with stronger reduction/oxidation abilities from each photocatalyst, quenching electrons/holes with weaker reduction/oxidation potentials with redox mediators (Figure 5.6d) or by direct recombination of the weaker oxidative holes and reductive electrons (Figure 5.6e).[45–48] Similarly, the vectorial electron-transfer process can recombine less-reductive electrons from one semiconductor with less-oxidative holes of the other semiconductor *via* a solid-interface metal phase instead of redox mediators in solution (Figure 5.6f).[49] The advantages and disadvantages and some examples of Z-scheme and vectorial electron-transfer processes are well-explained in ref. 33.

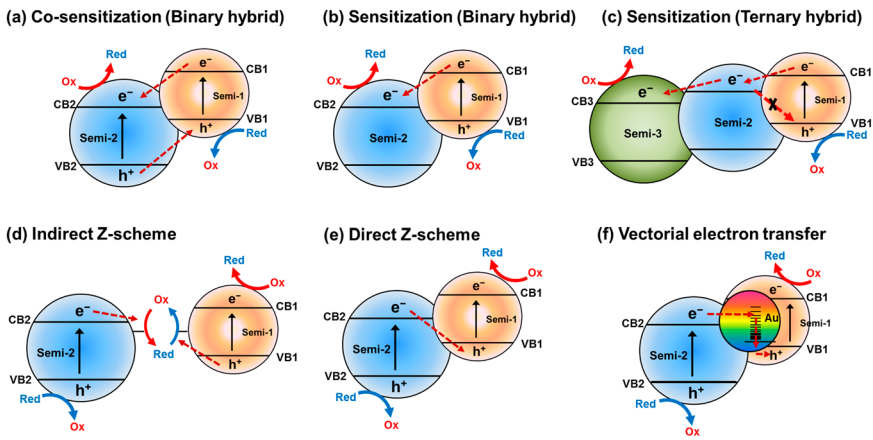

Figure 5.6 Schematics of various electron transfers in several semiconductor composite systems: (a) co-sensitization, (b) sensitization in a binary hybrid, (c) sensitization in a ternary hybrid, (d) indirect Z-scheme, (e) direct Z-scheme, and (f) vectorial electron transfer.

5.4 Dye-Sensitized Semiconductors and Dye Discoloration

Dye sensitization has mainly focused on the effective absorption of visible light to enhance the photo-conversion efficiency; its operation mechanism is conceptually similar to that of dye-sensitized solar cells (DSSCs).[50–52] Amongst the various dyes (*i.e.*, organic, inorganic, organometallic complexes, *etc.*) that have redox properties and visible light sensitivity, ruthenium complexes such as $Ru(dcbpy)_2$, $Ru(dcbpy)_2(NCS)_2$, and $[Ru(dcbpy)_2(dpq)]^{2+}$ (where dcbpy = 4,4′-dicarboxy-2,2′-bipyridine and dpq = 2,3-bis(2′-pyridyl)quinoxaline) have been widely utilized as sensitizers.[53–59] In principle, electron transfer in dye-sensitized semiconductor systems is very rapid and highly efficient. For the TiO_2–$Ru(dcbpy)_2(NCS)_2$ system, the photogenerated electron can be transferred from excited dyes to the CB of TiO_2 through two pathways in which both singlet and triplet excited states exist in $Ru(dcbpy)_2(NCS)_2$: one pathway involves the direct transfer of electrons from a singlet metal to ligand charge transfer (^{1}MLCT) excited state to the CB of TiO_2 (Figure 5.7a, Channel A), and the other involves the indirect transfer of electrons from a triplet metal to ligand charge transfer (^{3}MLCT) to the CB of TiO_2 (Figure 5.7a, Channel D) followed by electron transfer from the excited ^{1}MLCT to the excited ^{3}MLCT (Figure 5.7a, Channel B) and then relaxation from the excited ^{3}MLCT to the lowest ^{3}MLCT state (Figure 5.7a, Channel C). Indirect electron transfer is known to be much slower than direct electron transfer, and dyes in which the lowest ^{3}MLCT state has a higher energy level than the CB edge of TiO_2 are expected to induce effective electron injection and high energy-conversion efficiency.[60] The electron-injection kinetics can be also affected by

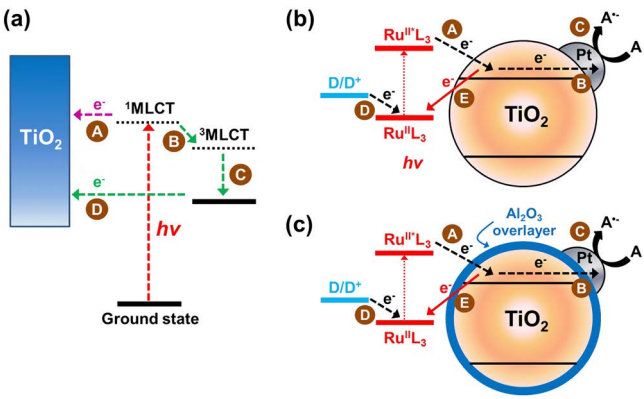

Figure 5.7 (a) Diagram of two-state electron (^{1}MLCT and ^{3}MLCT) injection of $Ru(dcbpy)_2(NCS)_2$ to the CB of TiO_2. (b) Visible light-induced photocatalytic reaction on a ruthenium complex-sensitized Pt/TiO_2 particle.[56] (Copyright 2014 American Chemical Society.) (c) Schematic illustration of a dye-sensitized TiO_2 particle with an Al_2O_3 overlayer. (Adapted with permission.[65] Copyright 2014 American Chemical Society.)

the binding distance and geometry between a sensitizer and semiconductor. As CH_2 spacer groups are introduced between the bipyridine and carboxylate groups in $Re(dcbpy)(CO)_3Cl$ complexes, the electronic coupling strength to TiO_2 is exponentially reduced, which reduces the electron-transfer rate.[61] Moreover, replacing the carboxylate anchoring groups in $Ru(dcbpy)_2$ with phosphonic ones markedly enhances the photocatalytic activity and stability over a wide pH range because of strong complexation with TiO_2.[62] To increase the photocatalytic efficiency, rapid electron injection is highly desirable and the reverse reaction between the injected electron and oxidized dye should be effectively inhibited. Although the electron injection rate is much faster than the recombination rate, the latter is predominant especially when nanoparticulate photocatalysts are isolated in suspension. Therefore, along with the development of new dyes to increase visible-light absorption and the electron-injection efficiency, some strategies to solve this issue have been investigated. As shown in Figure 5.7(b) and (c), loading of noble metals as a co-catalyst on TiO_2 and surface passivation of TiO_2 using an alumina overlayer effectively prohibits the recombination process (Channel E).[63–65] The electrons that are injected from the excited dyes to the CB of TiO_2 and their further transfer to the acceptors (*e.g.*, H^+, O_2, CCl_4, CCl_3COOH, Cr(VI)) initiates redox reactions under visible light irradiation. The time-resolved diffuse reflectance spectra of slurry-type TiO_2 and Al_2O_3/TiO_2 confirmed that the recombination of the electron injected from the excited dye with the oxidized dye was effectively retarded by the surface passivation. A very thin overlayer of alumina did not significantly affect the yield of electron injection from the excited dye to the TiO_2 CB despite being an insulator.

In the absence of sacrificial reagents, such as I^{3-}/I^- pairs[53] and EDTA,[56] dyes tend to be self-degraded by the remaining holes because electron transfer from water requires a high overpotential (Figure 5.7b and c, Channel D). Accordingly, regeneration of the dyes is essential to sustain the reaction cycles. From the environmental perspective, the treatment of industrial dyestuffs in wastewater is an important issue because they are toxic. Dye-sensitized TiO_2 systems can also be applied to discoloration of dye molecules and further mineralization to CO_2 *via* reactive oxygen species (ROS) or by direct degradation after sensitization. In principle, the transfer of electrons from the exited dye to oxygen (Figure 5.7b and c, Channel A → B → C) generates superoxide anions, and further electron transfer produces hydrogen peroxide, which is a source of hydroxyl radicals with strong oxidizing power. In a Pt/TiO_2 system, the excellent catalytic property of Pt for the reduction of dioxygen enhances the generation of ROS ($O_2^{-\bullet}$, H_2O_2, $HO^\bullet$, *etc.*), which accelerates the dye decomposition.[66] In general, the decolorization of organic dyes is relatively efficient in most dye-sensitized TiO_2 systems. However, the decolorization indicates only the destruction of the chromophoric groups of dyes, not the complete mineralization of dye molecules.[67] Even after complete dye decolorization, the degradation intermediates with toxicity persist.[68] As a result, the mineralization of dyes should be monitored by measuring chemical oxygen demand (COD), total organic carbon (TOC), total CO_2 emission, or the formation of inorganic ions.[68–70]

5.5 LMCT-Sensitized Semiconductors

One approach to extend the light response of wide band-gap semiconductors such as TiO_2 into the visible region is LMCT sensitization. This process results in visible light inducing charge transfer from the ground state of the adsorbate to the CB of the semiconductor. Figure 5.8 compares typical dye sensitization with LMCT sensitization.[71] Dye sensitization involves the absorption of visible light *via* HOMO–LUMO photoexcitation of dye molecules, which are pre-adsorbed onto the surface of the semiconductor; the photoexcited electron is then transferred from the dye to the semiconductor CB, and the oxidized dye is usually regenerated in the presence of suitable electron donors (Figure 5.8a). In contrast, in LMCT sensitization, the light initiates a direct electron transfer from the HOMO of the adsorbate (without involvement of the LUMO of the adsorbate) to the CB of the semiconductor. The oxidized adsorbate, which still contains a hole, could be further degraded or regenerated in the presence of a suitable electron donor as in the case of dye sensitization (Figure 5.8b).[71]

In LMCT sensitization, the HOMO level of the adsorbate is a critical factor in determining the extension of the light absorption range of the semiconductor. If there is strong coupling between the molecular orbital of the adsorbate and the energy band of the semiconductor, a new absorption band could appear that is not evident in either the adsorbate or semiconductor alone. This implies that LMCT sensitization has a significant potential for the development of cheap visible light sensitizers. Unlike dye sensitization, which requires that the sensitizer itself absorbs visible light, various inexpensive organic/inorganic compounds that have suitable HOMO levels can possibly form LMCT complexes that absorb visible light on the surface of wide band-gap semiconductors.[65] This process is particularly advantageous

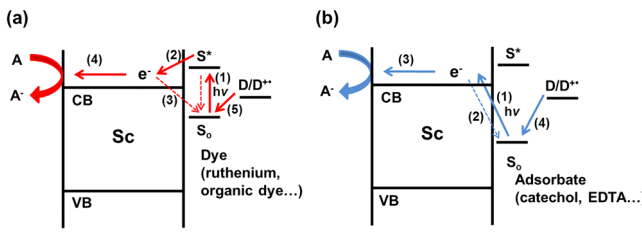

Figure 5.8 Schematic illustration of two similar visible light-sensitization techniques for wide band-gap semiconductors. (a) Dye sensitization: (1) HOMO–LUMO excitation of the dye, (2) electron transfer from the excited state of the dye to the semiconductor CB, (3) recombination, (4) electron transfer to the acceptor, and (5) regeneration of the dye by an electron donor. (b) LMCT sensitization: (1) visible light-induced LMCT, (2) recombination, (3) electron transfer to the acceptor, and (4) regeneration of adsorbates by an electron donor. S_0 and S* represent the ground and excited states of the sensitizer/adsorbate, respectively. (D: electron donor, A: electron acceptor.) (Adapted with permission.[71] Copyright 2014 The Royal Society of Chemistry.)

for the degradation of organic pollutants because numerous organic pollutants (*e.g.*, phenol) can form LMCT complexes on the surface of wide band-gap semiconductors and self-degrade under visible-light illumination.[72–74]

For LMCT sensitization, an adsorbate should form a complex on the surface of the semiconductor. Therefore, the surface sites of semiconductor are important. It was reported that some enediol ligands such as dopamine and catechol have a strong affinity for under-coordinated surface sites of TiO_2.[75] The authors suggested that the deepest surface sites are the most reactive toward binding of the enediol ligands, and the binding of ligand shifts the energy of surface sites toward the CB of TiO_2. The kind of functional groups on the adsorbate molecule is another important parameter for LMCT sensitization, which is critical in the formation and applications of LMCT complexes. Several compounds with different linkages have been examined for LMCT sensitization; for example, organic compounds with phenolic (*e.g.*, catechol), carboxylic (*e.g.*, oxalic acid), and hydroxyl (*e.g.*, cyclodextrin) linkages have been reported to form LMCT complexes on the surfaces of semiconductors, and most of them were studied for the self-degradation of LMCT complexes.[76–79] Because LMCT complexes that are anchored onto semiconductor surface through a functional group are not stable enough, LMCT complexes with multiple anchoring bonds have been studied. Zhang *et al.* reported LMCT complexation between TiO_2 and a phenolic resin (PR), which forms a strong complex through multiple anchoring groups; this complex exhibited visible-light activities for H_2 production from water and the degradation of organic pollutants (Figure 5.9).[80] LMCT sensitization can also be achieved with inorganic linkages; for example, LMCT complexes with cyanide or isocyanate linkages have been reported and can possibly be used as stable visible-light photocatalysts.[81–83] Hydrogen peroxide can also form an LMCT complex on the surface of a semiconductor through its hydroxyl

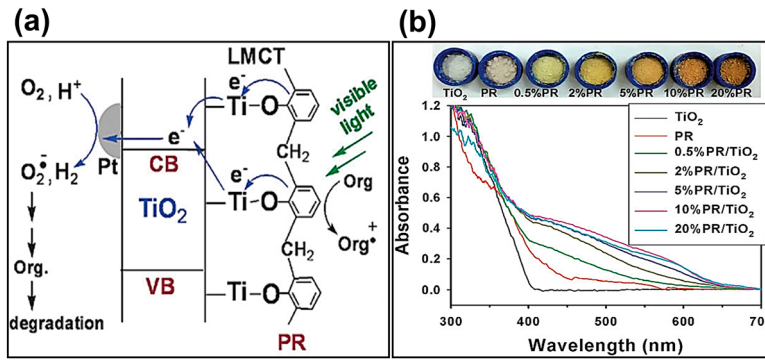

Figure 5.9 (a) Schematic illustration of the proposed electron-transfer pathways on PR–TiO_2 for H_2 production and degradation of organics under visible light (PR, phenolic resin). (b) UV/visible spectra of TiO_2, PR, and PR–TiO_2 samples. The upper photo shows the color changes induced by PR complexation on TiO_2. (Adapted with permission.[80] Copyright 2012 The Royal Society of Chemistry.)

linkage and could generate a hydroxyl radical that would mineralize pollutants under visible light.[84] LMCT sensitization is even possible through physisorption, which is different from most LMCT complex systems that are typically based on chemisorption. For instance, Seo *et al.* reported that pure polycyclic arenes can form LMCT complexes with dry TiO_2 surfaces and the resultant colored arene–TiO_2 complex could be reversibly bleached without degrading the arene compounds.[85]

Extension of the light response of wide band-gap semiconductors through LMCT sensitization should be useful considering the variety of organic/inorganic compounds that could potentially form LMCT complexes, while the more popular dye-sensitization method requires efficient dyes that are often expensive and unstable. However, most LMCT-sensitization studies that have been reported to date are based on a TiO_2 system and their solar conversion efficiency should be improved. Generally, the solar conversion efficiencies of LMCT complexes have not reached those of dye-sensitized TiO_2 or UV–TiO_2 systems.

5.6 Photoexcitation at Metal/Semiconductor Interfaces

The efficiency of a semiconductor photocatalyst is generally limited by two critical issues: (i) low light absorption because of the wide band-gap of the semiconductor and (ii) fast electron–hole pair recombination. A useful approach to overcome these problems is coupling semiconductor photocatalysts with metal nanoclusters. In principle, loading of metal nanoclusters onto a wide band-gap semiconductor provides three potential benefits: firstly, metal nanoclusters on the surface of the semiconductor can act as electron traps and form Schottky junctions, which facilitate the separation of photo-exited electron and holes in the semiconductor.[86] This process is useful for reducing electron–hole pair recombination and enhancing the photocatalytic activity of semiconductors. Secondly, metal nanoclusters can act as co-catalysts that lower the overpotentials for various photochemical redox reactions; for example, Pt nanoclusters are excellent co-catalysts that can greatly improve the photocatalytic H_2 production efficiency.[4] Lastly, metal nanoclusters can be sensitizers that harvest visible light through local surface plasmon resonance (LSPR). In this section, we focus on visible-light absorption and the photocatalytic activity of plasmonic photocatalysts.

LSPR of metal nanoclusters refers to the optical phenomenon in which the conducting electrons on the metal nanoclusters in resonance with the electrical field of incoming light undergo coherent oscillation.[86] When the light is illuminated onto metal nanoclusters that are smaller than the incident wavelength, some of the photons are scattered and some are absorbed through LSPR. The resonant frequency of LSPR is strongly dependent on the size, shape, and configuration of the plasmonic photocatalyst. For example, the LSPR of Au nanoparticles, which are one of the most widely

investigated noble metal nanoparticles for LSPR, can be tuned by changing the shape of the Au metal nanocluster. Gold nanoparticles have a single absorption band at ~530 nm, while Au nanorods have two bands; this is attributed to the presence of two separate plasmon bands along the short and long axes of the rod-shaped Au nanocluster.[87–89] As the aspect ratio (*i.e.*, length-to-width ratio) of the Au nanorod increases, the LSPR wavelength is redshifted (Figure 5.10a). The LSPR behaviors of metal nanoclusters are also affected by the morphology of the metal/semiconductor hybrid system. Seh *et al.* investigated the electric near-fields of two Au/TiO_2 systems with symmetric core–shell (Figure 5.10b) and non-centrosymmetric Janus (Figure 5.10c) structures.[90] The Janus Au/TiO_2 induces strong non-centrosymmetric localization of the plasmonic near-fields close to the Au–TiO_2 interface, which leads to improved optical absorption and enhanced photocatalytic activity relative to that of the core–shell Au/TiO_2 system under visible light.

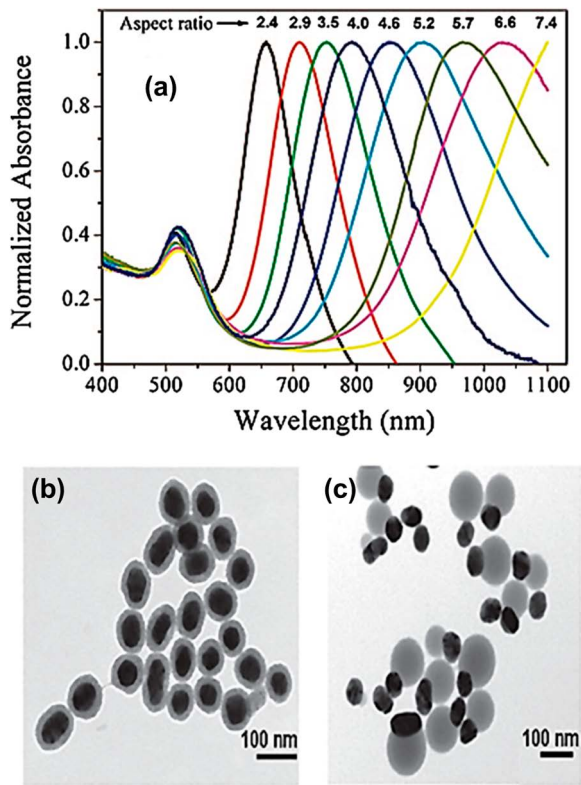

Figure 5.10 (a) LSPR wavelengths of Au/TiO_2 nanorods that were tuned by controlling the aspect ratio. (Adapted with permission.[89] Copyright 2008 American Chemical Society.) TEM images of (b) core–shell and (c) Janus Au/TiO_2 nanostructures. (Adapted with permission.[90] Copyright 2012 John Wiley & Sons.)

Several plasmonic photocatalysts consisting of noble metals (*i.e.*, Au, Ag, and Pt) and semiconductors (*i.e.*, TiO_2, AgCl, AgBr, and AgI) have been prepared and applied for water splitting, organic degradation, and reduction of Cr(VI) under visible light.[91–95] Figure 5.11 schematically illustrates the traditional view of the charge-transfer pathways in metal/semiconductor hybrid systems under visible-light illumination. Photocatalytic water splitting with Au/TiO_2 under visible light was chosen as an example.[96] Unlike the case of UV irradiation in which the Au nanoparticles act as both an electron reservoir and a co-catalyst for H_2 production, the Au nanoparticles under visible-light irradiation act as a visible-light sensitizer through LSPR. The electrons from Au are injected into the CB of TiO_2, which induces the generation of H_2 and the oxidation of electron donor (*e.g.*, EDTA) (Figure 5.11a). In the presence of a sacrificial electron acceptor such as $AgNO_3$, the holes located in certain Au nanoparticles with high oxidizing abilities can oxidize water (Figure 5.11b). Through a similar charge-transfer mechanism, the photocatalytic reactions of plasmonic photocatalysts for organic degradation can also occur under visible-light irradiation.[97–99]

In the above mechanism, the transfer of electrons occurs only when the energy of the excited electron in the metal is higher than that of the semiconductor CB edge. However, the charge separation at the interface can also be enabled through an alternative mechanism in which the charge separation occurs immediately upon photoexcitation. According to Long *et al.*, in about 50% of cases, an electron appears inside TiO_2 immediately upon photoexcitation because the plasmon excitation exhibits a strong delocalization into

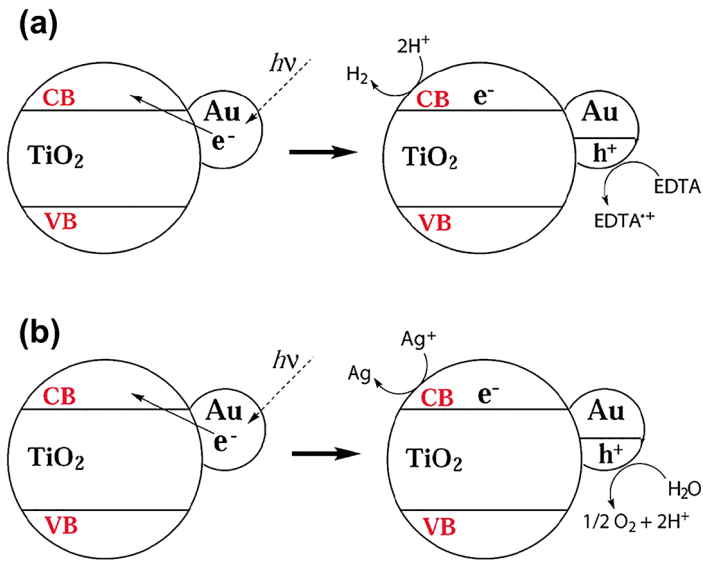

Figure 5.11 Proposed photocatalysis mechanisms of Au/TiO_2 upon excitation through LSPR for (a) H_2 generation and (b) O_2 evolution under visible light. (CB, conductance band; VB, valence band.) (Adapted with permission.[96] Copyright 2011 American Chemical Society.)

TiO_2.[100] In the remaining 50% of cases, the plasmonic excitation generates electron–hole pairs inside the Au nanoparticle and the electron is transferred to the TiO_2 surface. In either case, close contact between the metal nanocluster and semiconductor is essential for transfer of the LSRP-induced electron.[86] The metal/semiconductor interface facilitates separation of the photogenerated electron–hole pairs and reduces recombination. The sizes and shapes of the metal nanoclusters determine the light-absorption range of LSPR and should be chosen to maximize the efficiency of the metal/semiconductor hybrid system.

5.7 Conclusions

The photoexcitation of a semiconductor is a prerequisite step for initiating the photocatalytic conversion process and various modification techniques have been developed to extend the light absorption by wide bandgap semiconductors (*e.g.*, TiO_2) to the visible light region. In this chapter, we introduced the principles and strategies of five common modification methods in relation to their effects on the semiconductor photoexcitation, which includes (1) impurity doping, (2) coupling with narrow band-gap semiconductor, (3) dye sensitization, (4) LMCT sensitization, and (5) LSPR sensitization. Since each modification system is very different from other modified systems in their action mechanisms and operating conditions, the resulting effect of a specific modified semiconductor on its activity is hard to generalize. The effects of a modification method are often substrate-specific, reaction-specific, and experimental conditions-specific. For example, a modified semiconductor that exhibits a highly enhanced activity for the degradation of organic compounds might have little activity for the H_2 production reaction (and *vice versa*). Therefore, the modification of a semiconductor should be based on a comprehensive understanding of the overall photocatalytic process, and the target applications of a modified semiconductor should be carefully selected considering various factors such as the working reaction mechanism, the operating experimental conditions, the expected stability of the photocatalyst, and the estimated cost.

Acknowledgements

This work was supported by the Global Research Laboratory Program (2014K1A1A2041044) funded by the Korean government (MSIP) through NRF and the DGIST R&D Program of the Ministry of Science, ICT, and the Technology of Korea (15-EN-01).

References

1. M. R. Hoffmann, S. T. Martin, W. Choi and D. W. Bahnemann, *Chem. Rev.*, 1995, **95**, 69.
2. X. B. Chen, S. H. Shen, L. J. Guo and S. S. Mao, *Chem. Rev.*, 2010, **110**, 6503.

3. L. Jing, W. Zhou, G. Tian and H. Fu, *Chem. Soc. Rev.*, 2013, **42**, 9509.
4. A. Kudo and Y. Miseki, *Chem. Soc. Rev.*, 2009, **38**, 253.
5. H. Park, Y. Park, W. Kim and W. Choi, *J. Photochem. Photobiol., C*, 2013, **15**, 1.
6. H. Kim, J. Kim, W. Kim and W. Choi, *J. Phys. Chem. C*, 2011, **115**, 9797.
7. Y. Park, S. H. Lee, S. O. Kang and W. Choi, *Chem. Commun.*, 2010, **46**, 2477.
8. Y. Park, N. J. Singh, K. S. Kim, T. Tachikawa, T. Majima and W. Choi, *Chem.–Eur. J.*, 2009, **15**, 10843.
9. W. Kim, T. Tachikawa, H. Kim, N. Lakshminarasimhan, P. Murugan, H. Park, T. Majima and W. Choi, *Appl. Catal., B*, 2014, **147**, 642.
10. J. Kim, D. Monllor-Satoca and W. Choi, *Energy Environ. Sci.*, 2012, **5**, 7647.
11. Q. Wu, Q. Zheng and R. V. d. Krol, *J. Phys. Chem. C*, 2012, **116**, 7219.
12. T. Takata and K. Domen, *J. Phys. Chem. C*, 2009, **113**, 19386.
13. I. Nakamura, N. Negishi, S. Kutsuna, T. Ihara, S. Sugihara and K. Takeuchi, *J. Mol. Catal. A: Chem.*, 2000, **161**, 205.
14. A. W. Xu, Y. Gao and H. Q. Liu, *J. Catal.*, 2002, **207**, 151.
15. K. Nagaveni, M. S. Hegde and G. Mdras, *J. Phys. Chem. B*, 2004, **108**, 20204.
16. J. Schneider, M. Matsuoka, M. Takeuchi, J. L. Zhang, Y. Horiuchi, M. Anpo and D. W. Bahnemann, *Chem. Rev.*, 2014, **114**, 9919.
17. C. Wang, C. Bottcher, D. W. Banemann and J. K. Dohrmann, *J. Mater. Chem.*, 2003, **13**, 2322.
18. L. Q. Jing, X. J. Sun, B. F. Xin, B. Q. Wang, W. M. Cai and H. G. Fu, *J. Solid State Chem.*, 2004, **177**, 3375.
19. J. Z. Bloh, R. Dillert and D. W. Bahnemann, *ChemCatChem*, 2013, **5**, 774.
20. J. Z. Bloh, R. Dillert and D. W. Bahnemann, *J. Phys. Chem. C*, 2012, **116**, 25558.
21. R. Asahi, T. Morikawa, T. Ohwaki, K. Aoki and Y. Taga, *Science*, 2001, **293**, 269.
22. B. B. Lakshmi, P. K. Dorhout and C. R. Martin, *Chem. Mater.*, 1997, **9**, 857.
23. S. U. M. Kahn, M. Al-Shahry and W. B. Ingler Jr., *Science*, 2002, **297**, 2243.
24. Y. Park, W. Kim, H. Park, T. Tachikawa, T. Majima and W. Choi, *Appl. Catal., B*, 2009, **91**, 355.
25. W. Ho, J. C. Yu and S. Lee, *Chem. Commun.*, 2006, 1115.
26. R. Hahn, A. Ghicov, J. Salonen, V. P. Lehto and P. Schmuki, *Nanotechnology*, 2007, **18**, 105604.
27. A. Ghicov, J. M. Macak, H. Tsuchiya, J. Kunze, V. Haeublein, L. Frey and P. Schmuki, *Nano Lett.*, 2006, **6**, 1080.
28. W. Zhao, W. Ma, C. Chen, J. Zhao and Z. Shuai, *J. Am. Chem. Soc.*, 2004, **126**, 4782.
29. H. Irie, Y. Watanabe and K. Hashimoto, *J. Phys. Chem. B*, 2003, **107**, 5483.
30. K. S. Yang, Y. Dai and B. B. Huang, *J. Phys. Chem. C*, 2007, **111**, 12086.

31. K. S. Yang, Y. Dai, B. B. Huang and M. H. Whangbo, *J. Phys. Chem. C*, 2009, **113**, 2624.
32. Z. Lin, A. Orlov, R. M. Lambert and M. C. Payne, *J. Phys. Chem. B*, 2005, **109**, 20948.
33. M. Batzill, E. H. Morales and U. Diebold, *Phys. Rev. Lett.*, 2006, **96**, 026130.
34. N. Serpone, *J. Phys. Chem. B*, 2006, **110**, 24287.
35. Q. Wang, C. Chen, W. Ma, H. Zhu and J. Zhao, *Chem.–Eur. J.*, 2009, **15**, 4765.
36. M. K. Nowotny, L. R. Sheppard, T. Bak and J. Nowotny, *J. Phys. Chem. C*, 2008, **112**, 5275.
37. C. D. Valentin, G. Pacchioni, A. Selloni, S. Livraghi and E. Giamello, *J. Phys. Chem. B*, 2005, **109**, 11414.
38. X. Chen, L. Liu, P. Y. Yu and S. S. Mao, *Science*, 2011, **331**, 746.
39. A. Naldoni, M. Allieta, S. Santangelo, M. Marelli, F. Fabbri, S. Cappelli, C. L. Bianchi, R. Psaro and V. D. Santo, *J. Am. Chem. Soc.*, 2012, **134**, 7600.
40. G. Liu, L. Z. Wang, H. G. Yang, H. M. Cheng and G. Q. Lu, *J. Mater. Chem.*, 2010, **20**, 831.
41. W.-T. Sun, Y. Yu, H.-Y. Pan, X.-F. Gao, Q. Chen and L.-M. Peng, *J. Am. Chem. Soc.*, 2008, **130**, 1124.
42. Y. Bessekhouad, D. Robert and J. Weber, *J. Photochem. Photobiol., A*, 2004, **163**, 569.
43. R. Brahimi, Y. Bessekhouad, A. Bouguelia and M. Trari, *J. Photochem. Photobiol., A*, 2008, **194**, 173.
44. H. Kim, J. Kim, W. Kim and W. Choi, *J. Phys. Chem. C*, 2011, **115**, 9797.
45. M. Gratzel, *Nature*, 2001, **414**, 338.
46. K. Sayama, K. Mukasa, R. Abe, Y. Abe and H. Arakawa, *J. Photochem. Photobiol., A*, 2002, **148**, 71.
47. M. Higashi, R. Abe, A. Ishikawa, T. Takata, B. Ohtani and K. Domen, *Chem. Lett.*, 2008, **37**, 138.
48. X. W. Wang, G. Liu, Z. G. Chen, F. Li, L. Z. Wang, G. Q. Lu and H. M. Cheng, *Chem. Commun.*, 2009, 3452.
49. H. Tada, T. Mitsui, T. Kiyonaga, T. Akita and K. Tanaka, *Nat. Mater.*, 2006, **5**, 782.
50. G. Hodes, *J. Phys. Chem. C*, 2008, **112**, 17778.
51. W. R. Duncan and O. V. Prezhdo, *Annu. Rev. Phys. Chem.*, 2007, **58**, 143.
52. A. Hagfeldt, G. Boschloo, L. C. Sun, L. Kloo and H. Pettersson, *Chem. Rev.*, 2010, **110**, 6595.
53. B. O'regan and M. Gratzel, *Nature*, 1991, **353**, 737.
54. K. Gurunathan, P. Maruthamuthu and V. C. Sastri, *Int. J. Hydrogen Energy*, 1997, **22**, 57.
55. Y. Cho, W. Choi, C.-H. Lee, T. Hyeon and H.-I. Lee, *Environ. Sci. Technol.*, 2001, **35**, 966.
56. E. Bae and W. Choi, *J. Phys. Chem. B*, 2006, **110**, 14792.
57. H. Park and W. Choi, *Langmuir*, 2006, **22**, 2906.
58. A. Hagfeldt and M. Gratzel, *Acc. Chem. Res.*, 2000, **33**, 269.

59. K. B. Dhanalakshmi, S. Latha, S. Anandan and P. Maruthamuthu, *Int. J. Hydrogen Energy*, 2001, **26**, 669.
60. T. Pullerits and V. Sundstrom, From Biological to Synthetic Light-Harvesting Materials-The Elementary Steps, *Energy Harvesting Materials*, World Scientific Publishing Co., Singapore, 2005.
61. J. B. Asbury, E. Hao, Y. Q. Wang, H. N. Ghosh and T. Q. Lian, *J. Phys. Chem. B*, 2001, **105**, 4545.
62. E. Bae, W. Choi, J. W. Park, H. S. Shin, S. B. Kim and J. S. Lee, *J. Phys. Chem. B*, 2004, **108**, 14093.
63. E. Bae and W. Choi, *Environ. Sci. Technol.*, 2003, **37**, 147.
64. J. M. Warman, M. P. d. Haas, P. Pichat, T. P. M. Koster, E. A. v. d. Zouwen-Assink, A. Mackor and R. Cooper, *Radiat. Phys. Chem.*, 1991, **37**, 433.
65. W. Kim, T. Tachikawa, T. Majima and W. Choi, *J. Phys. Chem. C*, 2009, **113**, 10603.
66. W. Zhao, C. C. Chen, X. Z. Li, J. C. Zhao, H. Hidaka and N. Serpone, *J. Phys. Chem. B*, 2002, **106**, 5022.
67. C. C. Chen, W. H. Ma and J. C. Zhao, *Chem. Soc. Rev.*, 2010, **39**, 4206.
68. M. Stylidi, D. I. Kondarides and X. E. Verykios, *Appl. Catal., B*, 2004, **47**, 189.
69. F. L. Zhang, J. C. Zhao, T. Shen, H. Hidaka, E. Pelizzetti and N. Serpone, *Appl. Catal., B*, 1998, **15**, 147.
70. T. X. Wu, G. M. Liu, J. C. Zhao, H. Hidaka and N. Serpone, *J. Phys. Chem. B*, 1998, **102**, 5845.
71. G. Zhang, G. Kim and W. Choi, *Energy Environ. Sci.*, 2014, **7**, 954.
72. S. Kim and W. Choi, *J. Phys. Chem. B*, 2005, **109**, 5143.
73. A. G. Agrios, K. A. Gray and E. Weitz, *Langmuir*, 2003, **19**, 1402.
74. A. G. Agrios, K. A. Gray and E. Weitz, *Langmuir*, 2004, **20**, 5911.
75. L. de La Garza, Z. V. Saponjic, N. M. Dimitrijevic, M. C. Thurnauer and T. Rajh, *J. Phys. Chem. B*, 2006, **110**, 680.
76. Y. H. Wang, K. Hang, N. A. Anderson and T. Q. Lian, *J. Phys. Chem. B*, 2003, **107**, 9434.
77. G. Kim and W. Choi, *Appl. Catal., B*, 2010, **100**, 77.
78. N. Wang, L. Zhu, K. Deng, Y. She, Y. Yu and H. Tang, *Appl. Catal., B*, 2010, **95**, 400.
79. X. Zhang, F. Wu and N. Deng, *Catal. Commun.*, 2010, **11**, 422.
80. G. Zhang and W. Choi, *Chem. Commun.*, 2012, **48**, 10621.
81. Y. X. Weng, Y. Q. Wang, J. B. Asbury, H. N. Ghosh and T. Q. Lian, *J. Phys. Chem. B*, 2000, **104**, 93.
82. E. Vrachnou, M. Gratzel and A. J. McEvoy, *J. Electroanal. Chem.*, 1989, **258**, 193.
83. D. Jiang, Y. Xu, D. Wu and Y. Sun, *Appl. Catal., B*, 2009, **88**, 165.
84. Y. F. Rao and W. Chu, *Environ. Sci. Technol.*, 2009, **43**, 6183.
85. Y. S. Seo, C. Lee, K. H. Lee and K. B. Yoon, *Angew. Chem., Int. Ed.*, 2005, **44**, 910.
86. S. T. Kochuveedu, Y. H. Jang and D. H. Kim, *Chem. Soc. Rev.*, 2013, **42**, 8467.
87. N. R. Jana, L. Gearheart and C. J. Murphy, *Adv. Mater.*, 2001, **13**, 1389.

88. X. H. Huang, I. H. El-Sayed, W. Qian and M. A. El-Sayed, *J. Am. Chem. Soc.*, 2006, **128**, 2115.
89. P. K. Jain, X. H. Huang, I. H. El-Sayed and M. A. El-Sayed, *Acc. Chem. Res.*, 2008, **41**, 1578.
90. Z. W. Seh, S. Liu, M. Low, S.-Y. Zhang, Z. Liu, A. Mlayah and M.-Y. Han, *Adv. Mater.*, 2012, **24**, 2310.
91. H. Zhang, X. Fan, X. Quan, S. Chen and H. Yu, *Environ. Sci. Technol.*, 2011, **45**, 5731.
92. Z. W. Liu, W. B. Hou, P. Pavaskar, M. Aykol and S. B. Cronin, *Nano Lett.*, 2011, **11**, 1111.
93. Y. Bi and J. Ye, *Chem.–Eur. J.*, 2010, **16**, 10327.
94. Z. Zheng, B. Huang, X. Qin, X. Zhang, Y. Dai and M.-H. Whangbo, *J. Mater. Chem.*, 2011, **21**, 9079.
95. C. Hu, T. Peng, X. Hu, Y. Nie, X. Zhou, J. Qu and H. He, *J. Am. Chem. Soc.*, 2010, **132**, 857.
96. C. Gomes Silva, R. Juarez, T. Marino, R. Molinari and H. Garcia, *J. Am. Chem. Soc.*, 2011, **133**, 595.
97. W. B. Hou, Z. W. Liu, P. Pavaskar, W. H. Hung and S. B. Cronin, *J. Catal.*, 2011, **277**, 149.
98. E. Kowalska, O. O. P. Mahaney, R. Abe and B. Ohtani, *Phys. Chem. Chem. Phys.*, 2010, **12**, 2344.
99. S.-i. Naya, A. Inoue and H. Tada, *J. Am. Chem. Soc.*, 2010, **132**, 6292.
100. R. Long and O. V. Prezhdo, *J. Am. Chem. Soc.*, 2014, **136**, 4343.